DEPENDENCE OF THE FUNDAMENTAL FREQUENCIES OF T.E. PIEZOELECTRIC TRANSDUCERS ON INTRINSIC LOSSES AND EXTERNAL LOADING

San Emeterio, José Luis; Ramos, Antonio
Instituto de Acústica. C.S.I.C.
Serrano 144.
28006 Madrid.
Spain.
Tel. 91-5618806;
Fax: 91-4117651,
E-mail: jluis@ia.cetef.csic.es

ABSTRACT

Thickness extensional (T.E.) piezoelectric elements are the base of many broadband ultrasonic transducers for imaging and detection applications. The measurement of their electrical impedance as a function of frequency, using an impedance analyser, is the usual technique to evaluate piezoelectric transducer material properties as well as to analyse the characteristics of multilayer broadband transducers. Intrinsic mechanical, dielectric and piezoelectric losses, in addition with external mechanical loading (backing, matching, medium) modify the fundamental resonance (f_n , f_s , f_r), and antiresonance (f_a , f_p , f_m) frequencies. On the other hand, the peak frequencies of the emission, reception and pulse-echo ultrasonic working bands depend on these same aspects but they are also dependent on the external E/R electrical loading. In this paper, some of these dependencies of the fundamental frequencies are described and analysed by means of an accurate transmission line model.

INTRODUCTION

Different types of piezoelectric materials (ceramics, polymers and ceramic-polymer composites) are the base of thickness extensional (T.E.) piezoelectric resonators used in the manufacturing of wide band piezoelectric transducers for ultrasonic applications. Different parameters of loaded and unloaded piezoelectric resonators can be obtained from the measurement of their complex electrical impedance values. The electrical impedance curves and their associated characteristic frequencies and bandwidths can be related to material constants and to resonator and transducer parameters.

The electrical impedance values of unloaded piezoelectric resonators depend essentially on the internal mechanical, dielectric and piezoelectric losses (neglecting parasitic and holder effects). On the other hand, when the resonator is mechanically loaded in its mechanical ports, these external mechanical loads usually play a predominating role in the measured impedance values. In this paper, the characteristic frequencies f_n , f_s , f_r and f_a , f_p , f_m are defined according to the last IEEE Standard on Piezoelectricity. Some dependencies of these frequencies on internal losses

and external mechanical loads, as well as a general procedure for their evaluation, are here presented.

In ultrasonic pulse-echo applications, broadband piezoelectric transducers are driven by electrical "spikes" in order to radiate short ultrasonic pulses into the propagation medium which, after some reflection on mechanical impedance discontinuities, are received by the same emitter transducer. The Fourier transforms of the emitted and received ultrasonic pulses determine the working ultrasonic bands. In this paper, some dependencies, on the electrical and mechanical loads, of the peak frequencies of the emission, reception and pulse-echo working bands are also presented.

ONE-DIMENSIONAL MODELS, ELECTRICAL INPUT IMPEDANCE AND CHARACTERISTIC FREQUENCIES

One-dimensional modelling of broadband T.E. piezoelectric transducers has shown a good accuracy in the prediction of the overall performance of the transducers. From the piezoelectric constitutive equations, elastic wave propagation equations, and mechanical and electrical boundary conditions, bearing in mind that broadband T.E. piezoelectric transducers have the rare acoustic port closed with an attenuating material ("backing"), a 3x3 electromechanical matrix can be obtained. This electromechanical matrix relates the magnitudes present at the front mechanical port (force F_L and velocity v of the radiating surface) with the magnitudes present at the electrical port (Voltage V and intensity I across the transducer electrodes). Using the classical electromechanical analogies (mechanical force/electrical voltage, and velocity/electrical intensity) different electrical equivalent circuits can be derived from this electromechanical matrix, such as Mason, Redwood, KLM, or the approximate Butterworth-Van Dyke circuit. The KLM model [1] is used in this work for the evaluation of working ultrasonic bands in emission, reception and pulse-echo under different electrical loading conditions.

Either from the electromechanical matrix or from the exact one-dimensional equivalent circuits, an analytical expression can be obtained for the electrical input impedance of the piezoelectric transducer:

$$Z_{in}(\boldsymbol{w}) = \frac{1}{j\,\boldsymbol{w}C_0^S}\left(1 - \frac{k_t^2}{\boldsymbol{g}}\,\frac{2Z_0^2\,(1-\cos\boldsymbol{g}) - j(Z_L+Z_B)Z_0\,\mathrm{sen}\,\boldsymbol{g}}{(Z_0^2+Z_LZ_B)\mathrm{sen}\,\boldsymbol{g} - j(Z_L+Z_B)Z_0\cos\boldsymbol{g}}\right)$$

In the most general case, the material constants involved in the clamped capacitance C_0^S, the electromechanical coupling coefficient k_t , the propagation constant γ, and the characteristic impedance of the piezoelectric material Z_0 , will be complex in order to account for the internal mechanical, dielectric and piezoelectric losses. The mechanical loads are represented by the characteristic impedances of the backing material Z_B and the irradiated media Z_L .

The internal losses of the piezoelectric unloaded transducer ($Z_B = Z_L = 0$), are neglected in the majority of studies. This is an adequate assumption for many traditional applications of piezoelectric materials (i.e. quartz), but it is not adequate for broadband piezoelectric transducer elements. When these internal losses are neglected, there are only two frequencies of interest around an isolated resonance, the resonance frequency f_1 at which the electrical impedance becomes zero, and the antiresonance frequency f_2 at which the impedance becomes infinite. These ideal frequencies are defined in [2] as:

f_1 : lower critical frequency, maximum admittance (lossless)
f_2 : upper critical frequency, maximum impedance (lossless)

When internal losses are taken into account, there are three frequencies of interest near the admittance maximum:
f_s : Frequency of maximum conductance
f_n : Frequency of minimum impedance
f_r : Resonance frequency (zero susceptance)

and there are other three frequencies of interest near the impedance maximum:

f_p : Frequency of maximum resistance

f_a : Antiresonance frequency (zero reactance)

f_m : Frequency of maximum impedance

It should be noted that the definition of these frequencies is independent of type of transducer model used for their analysis, though computed frequency shifts depend on the model. We use these definitions for both loaded and unloaded resonators.

SOME DEPENDENCIES OF THE FUNDAMENTAL FREQUENCIES ON INTRINSIC LOSSES

The complex electrical impedance curves and the characteristic frequencies around the fundamental resonance are frequently used for the characterization of piezoelectric resonators. The internal losses play, in this case of unloaded transducer elements, a predominant role. The shifts of the fundamental frequencies f_s and f_p caused by intrinsic losses has been studied in previous papers [3-6], using as a reference the exact one-dimensional model with complex material constants for the account of losses. It was shown that, according to the adopted model, the increase of intrinsic mechanical losses increases the resonance frequency f_s, and decreases the antiresonance frequency f_p. It was also shown that the effects of dielectric losses on these characteristic frequencies are quite different than those produced by mechanical losses.

Figure 1 shows the evolution of these characteristic frequencies, f_s and f_p, with the mechanical loss tangent (tan δ_m), for different values of the dielectric loss tangent (tan δ_e), in the case of a low coupling coefficient resonator ($k_t = 0.15$).
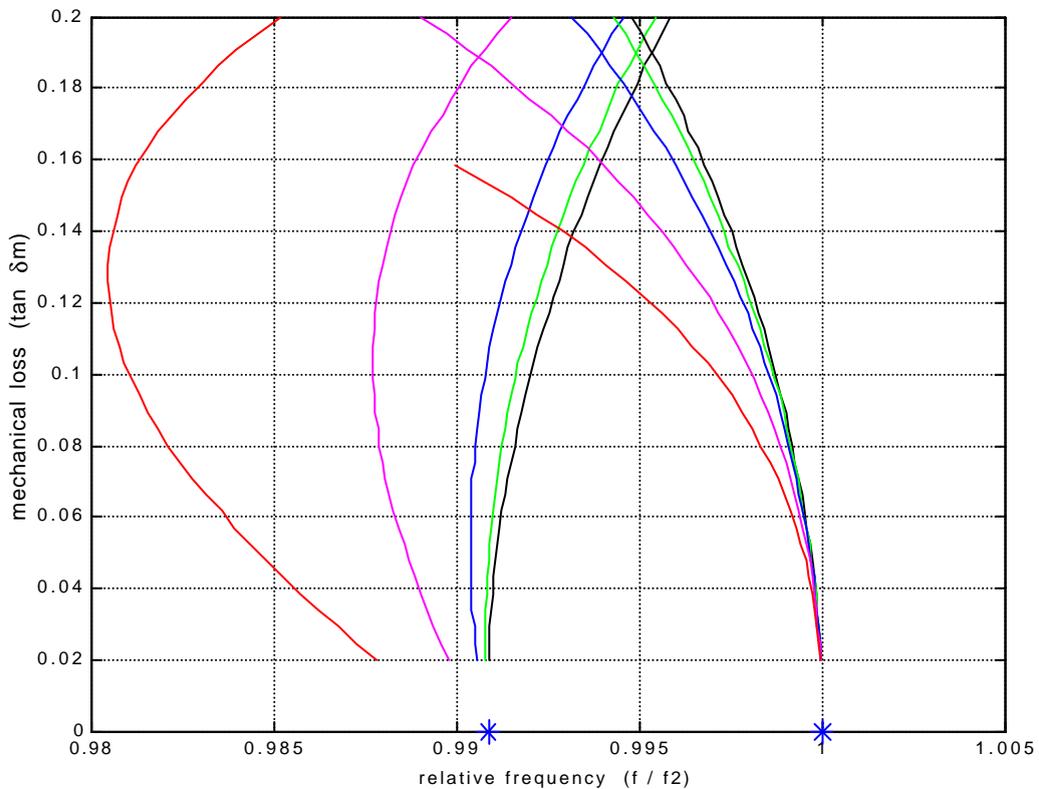
Figure 1. Shift of the frequencies f_s and f_p caused by the internal mechanical losses (tan δ_m) in the case of a low coupling coefficient resonator ($k_t = 0.15$). The asterisks locate the values of the lossless frequencies f_1 and f_2 . Different colours correspond to different values of dielectric losses:

a) black: tan δ_e = 0.001; b) green: tan δ_e = 0.01; c) blue: tan δ_e = 0.03; e) magenta: tan δ_e = 0.1; and f) red: tan δ_e = 0.25

The dependences of the other characteristic frequencies with internal mechanical and dielectric losses have also been computed. As a brief summary, it can be said that the frequency f_n decreases with the increasing of mechanical losses, while on the contrary f_m increases. For a high value of mechanical losses, the frequencies f_s and f_a disappear, because there are not points of zero susceptance or zero reactance around the fundamental resonance.

These frequency shifts have been computed by the following procedure: the normalized electrical impedance of the piezoelectric resonator [6] is computed in the relative frequency interval (0.7 − 1.2)f_2 at 20000 equally spaced data points. From the resulting complex impedance values, the corresponding maximum, minimum, and zero crossing points and frequency values are determined.

SOME DEPENDENCIES OF RESONANCE FREQUENCIES ON EXTERNAL MECHANICAL LOADING

T.E. piezoelectric plates used in the fabrication of broadband transducers are usually backed by an attenuating material of acoustic impedance Z_B in order to obtain a shortening in the ultrasonic pulses, broadening their bandwidths. In addition, the front face is loaded by the inspected medium (either directly or by means of matching layers) of acoustic impedance Z_L. In this case, the acoustic impedances Z_B and Z_L generally play a predominant role in the resulting values of the electrical impedance.

The normalized electrical impedance bands [6] and associated frequencies have been computed for two types of external mechanical loading: a) a symmetrical loading, with $Z_B = Z_L$; and b) an asymmetrical loading, assuming an air-backed transducer $Z_B = 0$, and varying Z_L from 0 to 12 Mrayls ($Z_L / Z_0 \cong 0.36$). A broadband transducer with the same characteristics of Q269 [7] has been considered, here and in the following section.
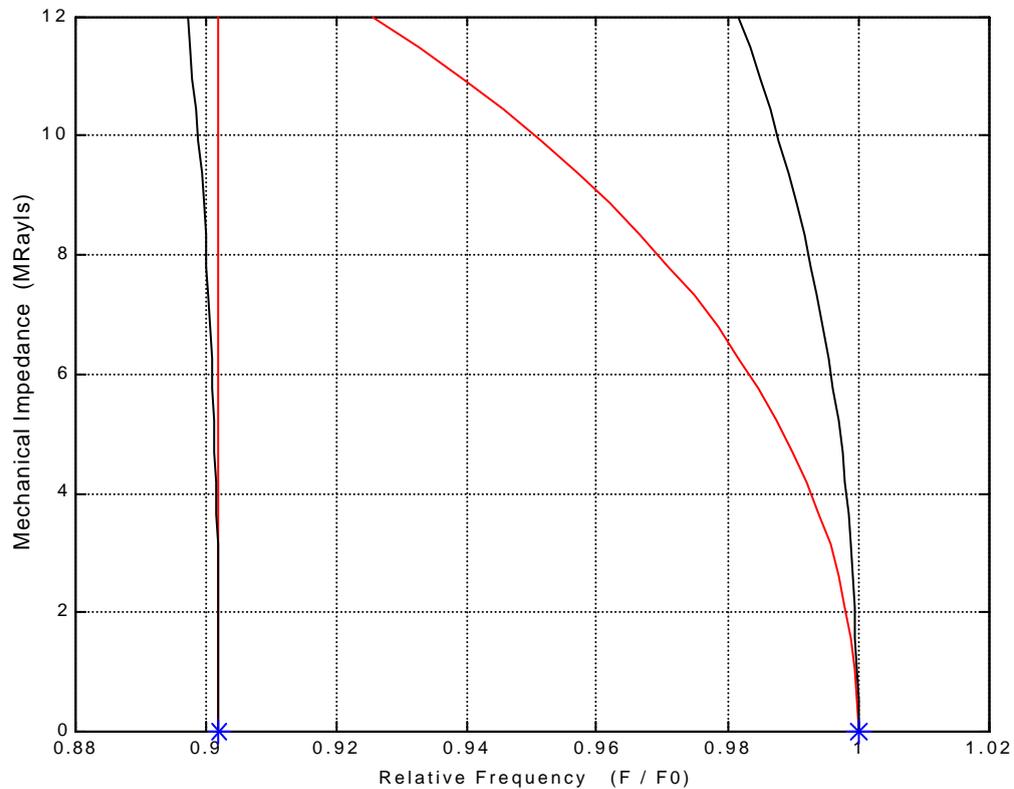
Figure 2. Shift of the frequencies f_s, and f_p caused by external mechanical loading. a) red, symmetrical loading $Z_B = Z_L$; b) black, asymmetrical loading $Z_B = 0$.

Figure 2 shows the evolution of the characteristic frequencies f_s and f_p with the mechanical loads. It can be observed how the frequency f_p decreases with the increase of the mechanical load in both cases of symmetrical and asymmetrical loading conditions. In the particular case of symmetrical loading, the frequency f_s is not modified by external mechanical loads. On the other hand, with asymmetrical load, the frequency f_s decreases with the increase of mechanical load. It should be noted that the shift of f_s caused by asymmetric external mechanical loading is opposite to the shift caused by internal mechanical losses.

SOME DEPENDENCES OF PULSE-ECHO FREQUENCIES ON EXTERNAL ELECTRICAL LOADING

Broad band piezoelectric transducers are electrically driven by means of "spikes" usually generated by capacitive-discharge electronic circuits, trying to obtain ultrasonic pulses of short duration looking for a good axial resolution. The frequency spectra of the radiated ultrasonic pulses and the received ultrasonic echo signals depend initially on the intrinsic losses and mechanical loading of the transducer. In addition, these frequency spectra depend on the electrical driving conditions[8], electrical matching networks [9], and characteristics of the reception electric stage [10]. The emission, reception and pulse-echo transfer functions, under different electrical matching conditions can be computed from the KLM model, using the T-matrix or "ABCD"-matrix formalism of circuit analysis [11].

Conventional approaches to the piezoelectric emission stage usually assume a waveform generator with resistive output impedance R_G. Figure 3.a shows the evolution of the peak frequency of the emission working band, as a function of R_G computed for different values of a parallel damping resistance R_D (for the same Q269 transducer). It should be noted that for an ideal voltage generator $R_G = 0$ (or when the emission transfer function is evaluated with reference to the transducer terminals), the peak frequency of the emission band tends to the frequency $f_s = 985295$ Hz of the loaded transducer. The increase of the internal resistance R_G of the generator produces an increase in the peak frequency, which approaches f_p in the absence of parallel damping. The use of a damping resistance R_D attenuates this frequency shift. The frequencies f_s and f_p of the loaded transducer ($Z_B = 5.4$ Mrayls; $Z_L = 1.5$ Mrayls) are marked by means of dashed lines.
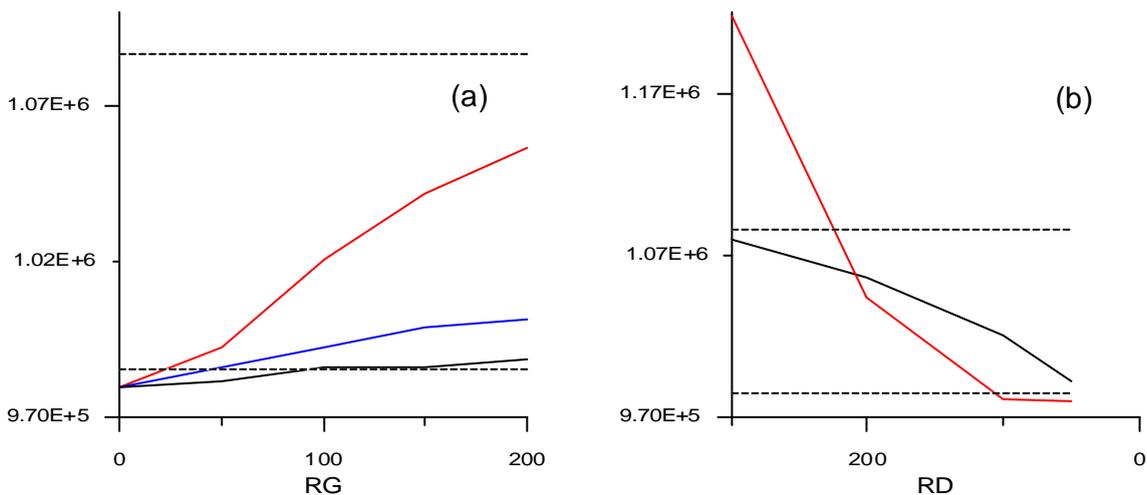
Figure 3. (a) Shifts of the peak frequencies of the emission working band as a function of generator output resistance R_G. i) red: without damping ($R_D = \infty$); ii) blue: $R_D = 100$ Ohms; iii) black: $R_D = 50$ Ohms. (b) Shifts of the peak frequencies of the reception working band as a function of the damping resistance R_D (at the origin of R_D axis there is not damping resistance, $R_D = \infty$). i) red: with inductive tuning coil $L_P = 22$ μH; ii) black: without inductive tuning.

The reception transfer function relates the voltage at the transducer electrical terminals with the mechanical force impinging the transducer front face. In the most simple case for displaying echo-signals, the transducer is connected to an oscilloscope, with an input resistance of at least 10 E6 Ohms. In this case, the peak frequency of the reception working band tends to the frequency f_p = 1086420 Hz of the loaded transducer. In order to increase the bandwidth and efficiency of the transducer, parallel tuning inductors and damping resistances are frequently used. When a damping resistance is used, the peak frequency of the reception band decreases, approaching f_s. as R_D decreases. Figure 3.b shows the evolution of the peak frequency of the reception working band, as a function of the damping resistance R_D, for two different electrical tuning situations: i) with a parallel tuning coil L_P = 22 µH; and ii) without tuning. It should be noted the extreme value of the peak frequency (1216800 Hz) in this last tuned case, at the origin of R_D axis ($R_D = \infty$), which is due to the existence of a double peak in the received frequency band.

The pulse-echo working band can be obtained by the product of the emission and reception frequency bands, and its peak frequency presents an intermediate behavior.

REFERENCES

(1) R. Krimholtz, F. Leedom, G. Matthaei, *New equivalent circuits for elementary piezoelectric transducers,* Electronic Letters, pp. 398-399 (1970)

(2) *IEEE Standard on Piezoelectricity*, ANSI/IEEE Std 176 (1987)

(3) J.L. San Emeterio, *Determination of electromechanical coupling factors of low Q piezoelectric resonators operating in stiffened modes*, IEEE Trans. on Ultrason., Ferroelec., and Frequency Control, Vol 44, Nº 1, pp. 108-113 (1997)

(4) J.L. San Emeterio, P.T. Sanz, A. Ramos, *Influence of dielectric losses on the shift of the fundamental frequencies of thickness mode piezoelectric ceramic resonators*. J. European Ceramic Society, Vol 19, (1999) pp. 1165-1169

(5) J.L. San Emeterio, *Influence of material damping on the shift of the resonance/antiresonance frequencies in thickness mode piezoelectric ceramic resonators*, Ferroelectrics , Vol 201, pp. 93-100 (1997)

(6) J.L San Emeterio, A. Ramos, P.T. Sanz, M. Cegarra, *Definition and measurement of the normalized electrical impedance of lossy piezoelectric resonators for ultrasonic transducers*, Ultrasonics, Vol. 38, pp. 140-144 (2000)

(7) A. Ramos, J.L. San Emeterio, P.T. Sanz, *Improvements in transient piezoelectric responses of NDE transceivers using selective damping and tuning networks*, IEEE Trans. on Ultrason., Ferroelec., and Frequency Control, Vol 47, Nº 4, pp. 826-835 (2000)

(8) Shafer and Levin. *Influence of front-end hardware on digital ultrasonic imaging,* IEEE Trans. Sonics & Ultrasonics, Vol. 31, Nº 4, pp. 815-826 (1987).

(9) A. Ramos, J.L. San Emeterio, P.T. Sanz, *Electrical matching effects on the piezoelectric transduction performance of a through-transmission pulsed process*, Ferroelectrics, Vol. 202, pp. 71-80 (1997).

(10) G. Hayward, *Using a block diagram approach for the evaluation of electrical loading effects on piezoelectric reception*. Ultrasonics, Vol. 24, No. 3, 1986, pp. 156-163.

(11) J.L. San Emeterio, A. Ramos, P .T. Sanz, A. Ruiz *Evaluation of impedance matching schemes for pulse-echo ultrasonic piezoelectric transducers*, Ferroelectrics (2002)